IOP Publishing | Astro Ltd Laser Physics

Laser Phys. **26** (2016) 084010 (20pp) doi:10.1088/1054-660X/26/8/084010

Laser technologies in ophthalmic surgery

V V Atezhev[1], B V Barchunov[1], S K Vartapetov[1], A S Zav'yalov[2], K E Lapshin[1], V G Movshev[2] and I A Shcherbakov[3]

[1] Physics Instrumentation Center, A.M. Prokhorov General Physics Institute, Russian Academy of Sciences, Moscow, Russia
[2] "Optosistemy", LLC, Moscow, Russia
[3] A.M. Prokhorov General Physics Institute, Russian Academy of Sciences, Moscow, Russia

E-mail: svart@pic.troitsk.ru

Accepted for publication 16 June 2016
Published 27 July 2016

Abstract

Excimer and femtosecond lasers are widely used in ophthalmology to correct refraction. Laser systems for vision correction are based on versatile technical solutions and include multiple hard- and software components. Laser characteristics, properties of laser beam delivery system, algorithms for cornea treatment, and methods of pre-surgical diagnostics determine the surgical outcome. Here we describe the scientific and technological basis for laser systems for refractive surgery developed at the Physics Instrumentation Center (PIC) at the Prokhorov General Physics Institute (GPI), Russian Academy of Sciences.

Keywords: laser technology, ophthalmic surgery, femtosecond lasers

(Some figures may appear in colour only in the online journal)

1. Introduction

One of the first branches of medical science, where lasers were used, was ophthalmology. The eye, with its transparent refractive media, was a perfectly convenient anatomical structure with the deep parts accessible for treatment by laser radiation and further monitoring of the results.

One of the first of such operations was laser coagulation by an argon laser, which provided an opportunity, for example, to fix retinal detachment to eye tunics. Another application of lasers was for glaucoma treatment, a disease caused by the stoppage of eye fluid outflow. In this case, the laser plays the role of 'a light needle' forming an artificial channel for this outflow.

These operations demonstrated the advantages of laser eye microsurgery such as

- non-contact
- being aseptic
- precise localization of the impact and minimal effect upon the neighboring tissues
- opportunity of surgery without violating the integrity of the eye's anatomic structures.

In ophthalmology, lasers found the broadest application for the correction of refractive errors. It was established in [1] that an excimer ArF laser with the wavelength 193 nm is optimal for corneal ablation according to the criteria of the ablation quantitative precision, the absence of any effect upon neighboring tissues, and the smoothness of the postsurgical surface. The first commercial excimer ophthalmosurgical setups operated with high-energy pulsed lasers and beams with characteristic dimensions equal to the diameter of the treatment field of the corneal optical zone (OZ) ($\leqslant$9 mm). The intensity profile at the cornea was formed by profiled rotating or changeable apertures. The first Russian commercial device [2] used an original optical scheme utilizing the Gaussian beam homogenizer. This formation technique provided an absolutely smooth postsurgical surface of the cornea. However, the application of wide-aperture beams did not provide an opportunity for stable correction of hyperopia and astigmatism. It was later proposed [3] that a small-diameter laser beam (0.7–1.2 mm) can be used to scan the corneal surface to form an arbitrary postsurgical surface. This technique is known as a 'flying spot'. Each pulse of an ArF laser ablates a small (smaller than 1 μm) corneal layer that provides an opportunity to form a calculated postsurgical surface with high precision.

The most modern type of laser ophthalmologic surgery is custom vision correction. The difference from the earlier techniques is that in the case of custom vision correction not only spheroastigmatic deviations get corrected, but also a patient's

Figure 1. (a) OZ is the optical zone, TZ is the transition zone, and UC is the intact (not ablated) cornea. (b) Composing parts of the OZ: OZ_0 is namely the optical zone and OZ_S is the suboptical zone.

unique nonregular refractive defects that cannot be corrected by spectacles. Custom correction is performed on the basis of keratometry (measurement of corneal shape) and aberrometry (aberration measurement for the whole eye's optical tract) data. Since in the case of custom surgery it is necessary to create smaller profile elements at the cornea, this surgery demands a new level of precision and stability for the laser correction of the corneal shape. In particular, the necessary element is an ***eye-tracking system*** for monitoring the surgical process that introduces corresponding corrections during surgery. The key parameter of the eye-tracking system is its ***latent period***, i.e. the time from the moment of eye displacement to the moment of registration of this movement during the surgery.

A human eye is a dynamic structure, where a multiplicity of processes with various time and space scales takes place. For example, eye movements during surgery must be considered with the time scale of milliseconds, while postsurgical adaptation processes may take several months. Each of these processes may affect decisively the quality of postsurgical vision and, therefore, must be taken into account while designing equipment for ophthalmologic surgery.

In this paper, we describe scientific and technological solutions implemented in commercial laser ophthalmosurgical systems 'MicroScan Visum' (an excimer laser) and 'Femto Visum' (a femtosecond (FS) laser) developed in PIC GPI, and also the results of the clinical use of these systems.

2. Excimer lasers

2.1. General issues of excimer-laser refractive correction

2.1.1. Pathologies as objects for treatment. In this paper, the refractive pathologies of vision are divided into regular (spheroastigmatic) and nonregular ones. It is assumed in both cases that the optical media of an eye stay completely transparent. ***Regular pathologies*** can be corrected by selecting standard spectacles that is equivalent to placing a spherical and cylindrical lens combination in front of an eye. All other refractive pathologies will be referred to as ***nonregular***. A special place among the latter belongs to ***presbyopia***, which is the loss of crystalline lens motility causing the impossibility of accommodation, i.e. control of an eye-focusing distance. A presbyopic patient has (using any kind of spectacles) only a very narrow range of distance, where he can see sharply.

Surgery for the treatment of regular refraction pathology is considered to be successful if the uncorrected distance visual acuity (UDVA) is no worse or better than the presurgery best corrected distance visual acuity (CDVA). In other words, if a patient has the visual acuity with spectacles equal to 1.0 before surgery, his visual acuity without spectacles after surgery must be 1.0 or better.

2.1.2. Basic techniques for diagnostics and postsurgical monitoring

A. ***Determination of subjective refraction*** (manual selection of spectacles). It provides an opportunity to determine the correction parameters for regular refractive distortions.
B. ***Keratotopography (keratometry).*** The basic output data are in the form (height map) of the outer surface of an eye cornea. Various types of curvature at each point of the cornea are calculated on its basis. Thus, the refractive properties of deep eye portions are not registrated by keratometry in any way.
C. ***Aberrometry*** provides information on the aberrations caused by not only defects of the cornea, but the whole optical tract of an eye. To measure these aberrations at the crossing point of the eye's optical axis and the retina, a small-sized infrared light source is formed that is obtained by directing a narrow beam along the eye's optical axis. In this case, the wavefront $W(x, y)$ leaving the pupil (in the form of an expansion over the Zernike polynomials [4]) represents the output data of an aberrometer. If a plane wavefront goes out of an eye focused at an infinitely distant object, in this ideal case the eye does not need surgical correction.

Thus, aberrometry provides not only geometrical, but optical data characterizing not only the cornea, but the whole optical tract. However, the definition domain of its data does not go beyond the pupil at the measurement moment, while the keratometry data are not restricted in this way.

2.1.3. Surgery classification in performance technique. A 50 μm layer of epithelium exists over the corneal surface layer. It must be removed before starting the laser treatment of the

cornea. Refractive surgery is divided into the following types according to the way it is performed.

A. Photorefractive keratectomy (PRK). The epithelium is removed mechanically.
B. Transepithelium PRK. The epithelium is removed by the same excimer laser that performs the major stage of the surgery.
C. LASIK (laser-assisted *in situ* keratomileusis). The epithelium is removed temporarily together with the corneal surface layer of 100–160 μm with the help of a mechanical instrument (microkeratom). After laser treatment of the cornea, the double-layer (cornea+epithelium) is placed back. This surgery type is most widely spread nowadays since it needs no special measures during the period of epithelium regeneration (about 3 days). The patient may continue with normal daily life immediately after the surgery.
D. Femto-LASIK. It is a modification of the LASIK technique, where the epithelium-corneal layer is formed by the action of an FS laser upon the cornea at a preset depth, with the upper surface layers of the cornea and the epithelium staying intact. The layer thickness is more uniform than in the case of the common LASIK technique and the interface is smoother.

2.2. Mathematical algorithms of ablation

We will use the terminological standard TOPS4 while describing the ablation algorithms. The standard was developed to describe aberrations of an eye's optical tract [5]. In particular, according to this standard, the coordinate center is positioned at the cross-section of the eye's optical axis with the outer surface of the cornea, the ***Oz*** axis selected to be co-directed with the eye's optical axis with the positive direction from the eye. The ***Ox*** axis is horizontal and directed to the left of the patient, and the ***Oy*** axis is directed upwards for the sitting patient.

The ablation profile (depth) was constructed proceeding from various principles, depending on the surgery type. The common issue for all surgery types was the presence of optical and transition ablation zones (figure 1(a)). In the optic zone (OZ) which is a circle with the center at the origin of the indicated coordinate system, the postsurgical corneal surface formed by a laser has the correct optical properties and is intended to form an image at the eye's retina. Evidently, the postsurgical surface of the cornea at the edge of the OZ, as a rule, will not be smoothly conjugated to the intact corneal surface. Therefore, it is necessary to construct a transition zone (TZ) between the OZ and the intact corneal zone, where the postsurgical surface formed by a laser will smoothly conjugate the surfaces in the optical and intact zones. For a smooth conjugation we require the continuity of the function $z = \boldsymbol{h_{postop}(x,y)}$ describing the postsurgical corneal surface and of its first derivatives over $\boldsymbol{x}$ and $\boldsymbol{y}$.

Below, we consider the ablation profile construction for different surgery types.

2.2.1. Standard type surgery. In this case, the parameters specifying the refractional correction to be made are the spheroastigmatic ones (Sph, Cyl, Axis) measured by clinical examination (selection of spectacles using Snellen-like tables). Calculation is based on the principles of geometrical optics.

Let us give some necessary definitions of the ophthalmometric terms.

A weak axis is the direction $\boldsymbol{O\alpha_{flat}}$ in the ***Oxy*** plane. It is the section of the presurgical cornea with a plane including the ***Oz*** axis and the $\boldsymbol{O\alpha_{flat}}$ beam (crossing the coordinate origin and constituting the angle $\boldsymbol{\alpha_{flat}}$ with the ***Ox*** axis) that has the minimum curvature (at the coordinate origin) among all directions $\boldsymbol{O\alpha}$ in the plane ***Oxy***.

A strong axis is the direction $\boldsymbol{O\alpha_{steep}}$ in the plane ***Oxy*** that is perpendicular to the weak axis.

The initial corneal surface was approximated by a sphere

$$z = h_{\mathrm{preop}}(x, y) = -R_{\mathrm{preop}} + \sqrt{R_{\mathrm{preop}}^2 - (x^2 + y^2)},$$

where the radius R_{preop} was calculated by the expression

$$R_{\mathrm{preop}} = (n_{\mathrm{a}} - 1)/(0.5^*(K_{1\mathrm{preop}} + K_{2\mathrm{preop}})).$$

Here, $K_{1\mathrm{preop}}$ and $K_{2\mathrm{preop}}$ are the ophthalmometric curvatures expressed in diopters for a presurgical cornea along the corresponding weak and strong axes and $\boldsymbol{n_a}$ is the average refractive index for the eye's optical media.

The target (surgery formed) surface of the cornea in this case was set as an ellipsoid

$$z = h_{\mathrm{postop}}(x', y') = -A_{z,\mathrm{postop}} - h_{\mathrm{shift}} + \sqrt{A_{z,\mathrm{postop}}^2 - ((x'/A_{x,\mathrm{postop}})^2 + (y'/A_{y,\mathrm{postop}})^2)}.$$

Here, $A_{x,\mathrm{postop}}$, $A_{y,\mathrm{postop}}$, and $A_{z,\mathrm{postop}}$ are the ellipsoid semi-axes and $h_{\mathrm{shift}} > 0$ is the additional depth shift necessary at certain combinations of parameters for spherocylindrical correction and also for forming a smooth geometry for the TZ. The coordinate system (x', y', z) is obtained from the coordinate system (x, y, z) by rotation of the ***Ox*** and ***Oy*** axes to the angle setting the direction of astigmatism correction.

The target ellipsoid parameters were calculated according to the standard principles of geometrical optics and differential geometry for 2D surfaces.

The ablation profile in the OZ was set by a formula

$$\mathrm{Abl}(x, y) = h_{\mathrm{postop}}(x, y) - h_{\mathrm{preop}}(x, y),$$

and in the TZ the ablation profile was constructed for each radius ($\varphi = \mathrm{const}$ in the polar coordinates) proceeding from the continuity condition for the ablation profile $\mathrm{Abl}(r, \varphi)$ and its first derivative $\partial\mathrm{Abl}(r, \varphi)/\partial r$ along this radius.

2.2.2. Correction with a conical constant. Correction with a conical constant (frequently called the 'Q-value') is generally conducted in the same way as the standard correction. The difference is the fact that the target postsurgical surface is not an ellipsoid, but the surface with the sections along the weak and strong meridians are conical curves.

For example, in the case of cylindrical symmetry, an equation for such a surface is

$$z = \frac{c(x^2 + y^2)}{1 + \sqrt{1 - (1 + k)c^2(x^2 + y^2)}},$$

where c is the curvature of the surface section at the coordinate origin and k is the conical constant.

In other aspects, construction of the ablation profile does not differ from standard type surgery.

Surgery with a conical constant was implemented for all types of spheroastigmatic correction and can be performed, in particular, for presbyopia correction.

2.2.3. Tissue-saving ablation. In the case of repeated surgery and also high levels of correction, frequently the problem of ablation depth minimization urgently arises. The simplest way to economize ablation is contraction of the OZ and TZ, but the results depend strongly on the correction type and, therefore, are hardly predictable.

A more correct way is to use multifocality. Namely, we proposed to separate within the OZ an exactly optical zone OZ_0 (the central circle concentric with the OZ circle) and a suboptical zone, i.e. the ring $OZ_S = OZ - OZ_0$ (figure 1(b)). The target postsurgical surface in the zone OZ_0 is formed as described for standard surgery, and in the zone OZ_S, proceeding from the fact that optical correction must be reduced in it to a preset value as a linear function of the radius.

2.2.4. Surgery based on corneal shape. This surgery type is conducted according to the data of keratometry, i.e. the measurement of the shape of the outer corneal surface. Namely, the output data of the keratotopograph are used: (1) a height map for the outer corneal surface in the form of a table; (2) the corneal curvatures ($K_{1\mathrm{preop}}$ and $K_{2\mathrm{preop}}$) along the strong and weak axes at the intersection point of the outer corneal surface with the eye's optical axis.

A standard spline interpolation of a table height map was performed to obtain a continuous presurgery surface of the cornea. The postsurgery surface was an ellipsoid as in the case of standard correction.

The ablation profile was constructed as the difference between the pre- and postsurgical surfaces. The ablation depth was increased by a constant, if this was necessary to form the TZ. A surgeon, in this case, sets spherocylindrical correction or directly indicates the curvatures ($K_{1\mathrm{postop}}$ and $K_{2\mathrm{postop}}$) for the postsurgical corneal surface along the weak and strong axes.

2.2.5. Surgery based on aberrometric data. Aberrometric data contain information on aberrations caused not only by corneal defects, but the whole eye's optical tract. To measure these aberrations, a small-sized infrared light source is formed at the intersection point of the eye's optical axis and the retina. This light source is made by directing a narrow beam along the eye's optical axis. The shape of a wavefront $W(x, y)$ going out of the pupil presented in the form of an expansion over the Zernike polynomials [1, 2] is exactly the output data of an aberrometer. If a plane wavefront goes out from an eye focused to an infinitely distant object, then in this ideal case the eye does not need surgical correction.

The OZ in the case of aberrometric correction coincides with the definitional domain for the Zernike polynomials which is the maximum-sized circle inscribed into the patient's eye pupil. The ablation profile in the OZ was set by a formula

$$\mathrm{Abl}(x, y) = (W(x, y) - w_{\mathrm{shift}})/(n_{\mathrm{cornea}} - 1) - h_{\mathrm{TZ,shift}},$$

where $w_{\mathrm{shift}} \geqslant 0$ is the minimal nonnegative number satisfying $W(x, y) - w_{\mathrm{shift}} \leqslant 0$ within the whole OZ and $h_{\mathrm{TZ,shift}} \geqslant 0$ is an additional depth increase, which may be needed to form a smooth TZ. Geometrical principles for the formation of the TZ, in this case, are identical to the ones used for standard type surgery.

A technique for OZ expansion. A problem specific to aberrometric type surgery is the small diameter of the OZ caused by the narrowing of the pupil, which may happen at the moment of aberrometry. We developed a technique for OZ expansion for this case. The technique is based on the separate calculation of ablation for correction of aberrations expressed by the Zernike polynomials of low (second) and high ($\geqslant$3) orders.

The principle of the proposed technique for OZ expansion is as follows. High-order aberrations have no physical sense beyond the definition domain for the Zernike polynomials, but their summary L_2-norm is usually small. At the same time, aberrations of low (second) order introduce the major contribution to ablation and have sense both within and beyond the Zernike circle (reflecting spherocylindrical correction). Therefore, the maximum OZ for high-order aberrations is the Zernike circle, while the OZ for low-order aberrations can be set wider, at the surgeon's discretion. The outer diameter of the TZ, in this case, was set the same for both types of aberrations.

Ablation, in this case, was expressed by the sum of the ablations for the aberrations of low and high orders.

$$\mathrm{Abl}(x, y) = \mathrm{Abl}_{\mathrm{LOA}}(x, y) + \mathrm{Abl}_{\mathrm{HOA}}(x, y).$$

By virtue of a relatively small contribution by higher orders into the summary value of ablation, this provides an opportunity to improve the quality of postsurgical vision, especially the quality of night vision (with an expanded pupil).

An ablation profile correction for ablation reduction in the case of deviation of laser beam incidence upon the cornea from the normal was introduced while calculating all surgery types [6].

2.3. Factors affecting the quality of laser-refractive correction

Surgery success, i.e. high quality of postsurgery vision, is determined by many factors. Insufficiently taking into account even one of these factors may reduce sharply the quality of life after surgery or even make a person disabled. The most important of these factors are listed below.

(1) ***Limitation of cornea thickness.*** The average cornea thickness is 550 μm, but it may vary depending on the race, nationality, sex, age and other factors. Different from the majority of body tissues, the cornea does not regenerate and, therefore, is an irreplaceable resource. A too thin (less than 250–300 μm) residual cornea may protrude under the effect of intraocular pressure. Therefore, in the case of the correction of high refractive anomalies, it is necessary to plan measures for ablation economy.

(2) ***LASIK-flap and PRK epithelization.*** An epithelial-corneal flap returned after LASIK surgery and epithelium regeneration after PRK surgery smoothe the postsurgical surface.

(3) ***Finiteness of the laser spot size*** means that the postsurgical shape of the cornea cannot be realized to absolute precision. On the other hand, the reduction of the spot diameter causes an increase in the number of laser pulses (inversely proportional to the square of the spot diameter) necessary for the surgery and an extended length of time taken for the surgery itself, which is undesirable for clinical considerations.

(4) ***Intrasurgery temperature of the cornea.*** Corneal overheating in the surgery process may deteriorate its optical properties.

(5) ***Surgical positioning relatively to the eye's optical axis, torsional orientation.*** The surgical zone center must coincide with the eye's optical axis and the surgical horizontal axis must coincide with that at the moment of diagnostic measurement. This is especially important for custom surgery, where the ablation profile includes small-sized elements.

(6) ***Motility and unstable visibility of the eye's anatomical structures.*** Geometrical linkage (both shift and torsion) is made according to the anatomical structures of an eye, i.e. a limb and an iris. The limb appearance may depend on the light conditions and the iris may unequally and irregularly contract during diagnostic measurements and in the surgical process.

(7) ***Stability of laser pulse energy.*** The higher the stability of the laser pulse energy, the higher is the probability of attaining preset postsurgical values for visual acuity. In the case of more than 1% variation in the laser pulse average energy during the operation, the reliability of attaining the target corneal surface (preset postsurgical refraction) is reduced considerably.

(8) ***Ratio of the eye pupil and ablation zone sizes.*** If the ablation zone is considerably smaller than the eye pupil, the visual quality may be reduced sharply. This problem is especially important for evening and night vision, i.e. under the conditions when the pupil is expanded.

(9) ***Quality of the TZ.*** Apart from mathematical smoothness, the TZ must secure the absence of the high values for the first and second spatial derivatives of the ablation profile within the whole region of the laser effect (OZ+TZ). The presence of sharp breaks and cuts will lead to unstable surgery results since it will cause the physiological smoothing of the ablation profile that in the case of LASIK surgery occurs on account of the flap action, and in the case of PRK, on account of an excessive increase of the corneal epithelium.

(10) ***Probability for unexpected interruption of surgery.*** In the case of sharp changes in the patient's general state, surgery must be stopped. This is a rare, but not improbable situation. Therefore, it is important to perform ablation in the order that will secure that in the case of surgery stopping, a patient will not have a wrong-shaped cornea that would complicate further completion of the surgical treatment.

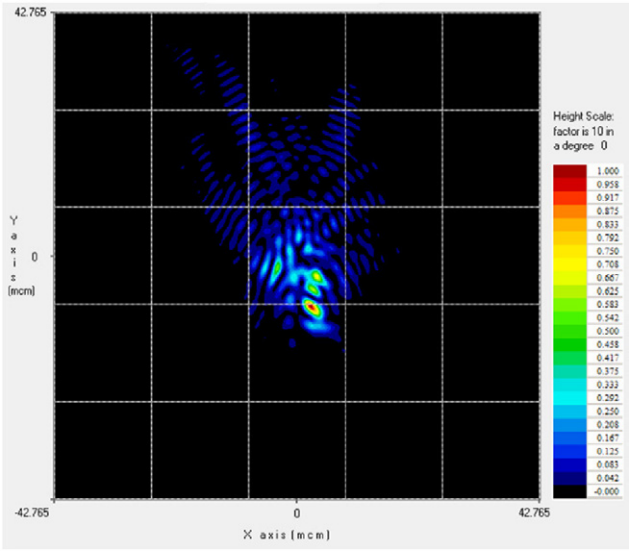

Figure 2. PSF calculated according to a patient's keratotopogram.

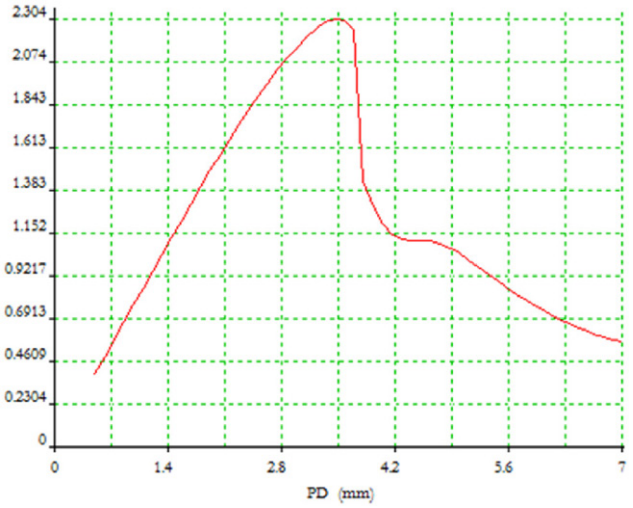

Figure 3. Dependence of vision acuity on the pupil diameter (PD) calculated according to a keratotopogram. (Visus = 1.0 corresponds to normal vision). One can see a sharp reduction in vision acuity at large PDs, i.e. for night vision. This reduction is typical in the presence of high-order aberrations.

2.4. An ophthalmologic excimer laser system 'Microscan Visum'

The above-listed factors are taken into account in the developed excimer laser system 'Microscan Visum' by a series of scientific and technological solutions, which are discussed below.

2.4.1. A mathematical model for an eye and surgery. A mathematical model for an eye and surgery was developed and implemented in the form of computer software (***a complete mathematical model for the eye's optical tract and surgery process***). This model provided

(i) calculation of an image at the eye retina (within the framework of wave optics) for a pupil with the diameter up to 7 mm; calculation of PSF (point spread function) and MTF

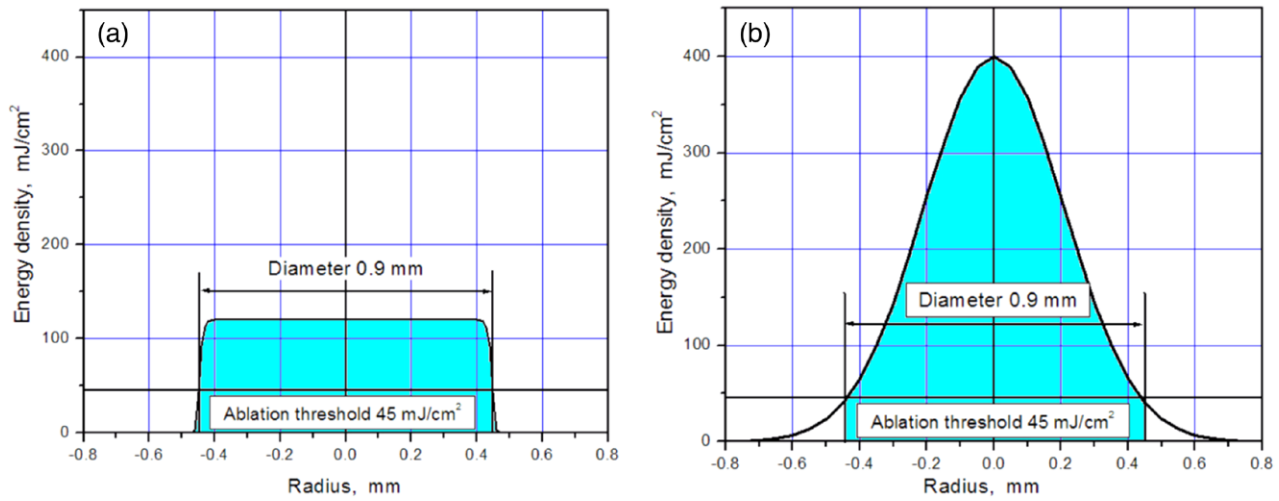

Figure 4. Comparison of ablation at (a) flat and (b) the Gaussian ablation profiles. (a) A flat beam. The maximum energy density is 120 mJ cm^{-2}. Pulse energy is 0.75 mJ. Ablation volume per pulse is 140 pl. Ablation depth per pulse is 220 nm. Ablation efficiency of 140/0.75 = 186 pl mJ^{-1}. (b) The Gaussian beam. The maximum energy density is 400 mJ cm^{-2}. Pulse energy is 1.5 mJ. Ablation volume per pulse is 200 pl. Ablation depth per pulse is 650 nm. Ablation efficiency of 200/1.5 = 133 pl mJ^{-1}.

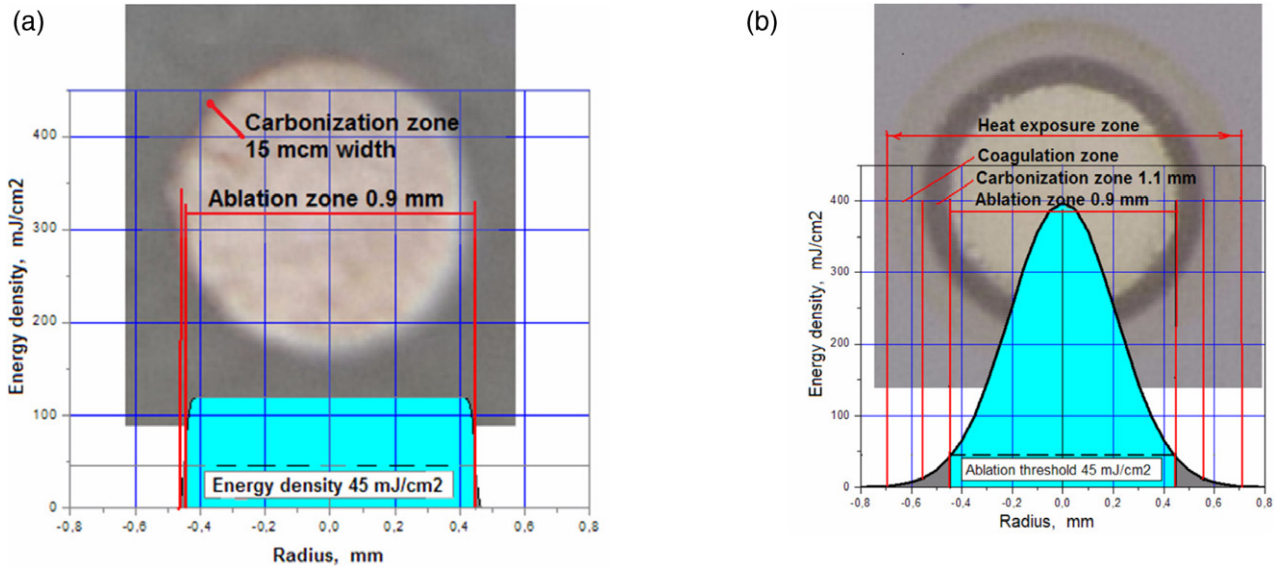

Figure 5. The photos of a PMMA plate after ablation at (a) flat and (b) Gaussian energy profiles in a laser spot. (a) A flat beam. Energy is750 nJ. Below the ablation threshold of 10–15 nJ. 1–2% of the total energy is spent on heating. (b) The Gaussian beam. Energy is 1500 nJ. Below the ablation threshold of 175 nJ. 11% of the total energy is spent on heating.

(modulation transfer function) according to kerato- and aberrograms. Figure 2 gives an example for calculating a PSF according to a patient's keratotopogram.

(ii) calculation of acuity for pre- and postsurgical vision according to the kerato- and aberrogram data. Figure 3 gives an example for calculating a vision-acuity PSF according to a patient's keratotopogram.

(iii) Simulation of the surgical process with taking into account intrasurgery motility of an eye, delays in the eye-tracking system, and variation of laser pulse energy. It was established that delays in the eye-tracking system do not worsen the quality of postsurgical vision if its latent period does not exceed 10 ms.

(iv) Simulation of LASIK flap and PRK epithelization effect upon the shape of the postsurgical surface and the postsurgical quality of vision. The flap effect was simulated by convolution of the corneal surface that was obtained after simulating ablation with the Gaussian kernel. The model was verified according to clinical data (pre- and postsurgical keratotopograms); the Gaussian kernel width at the level of half-height was 1.5 mm. This parameter turned out to be the same for the LASIK flap and PRK epithelization effects, but in the latter case the completion of the smoothing process (on account of epithelium growth) occurs much later (up to one month).

Thus, the model provided an opportunity to compare the expected and real changes in patient vision after surgery and reveal the admissible values for the system parameters. In complicated clinical cases (thin cornea, repeated surgery,

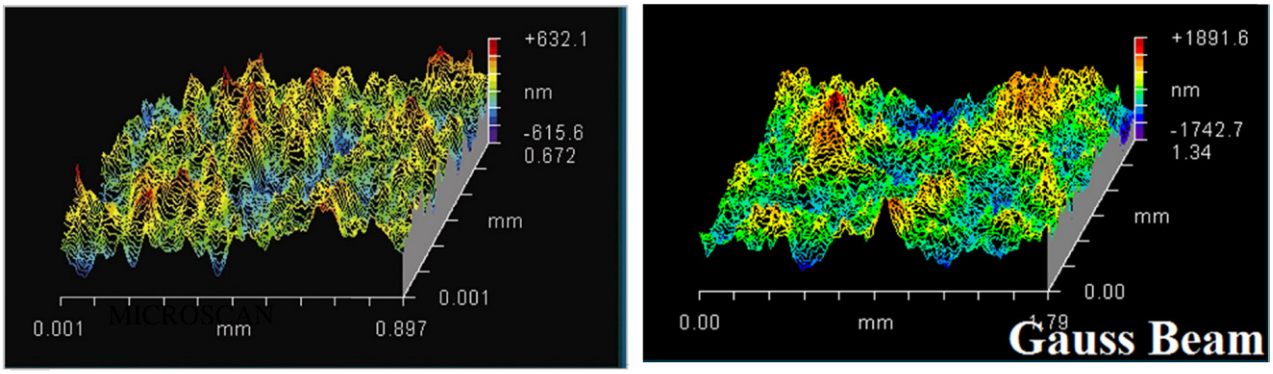

(a) (b)

Figure 6. The surface of a PMMA plate after ablation at (a) flat and (b) Gaussian energy profiles in a laser spot. (a) RMS = 192 ± 11 nm. (b) RMS = 455 ± 35 nm.

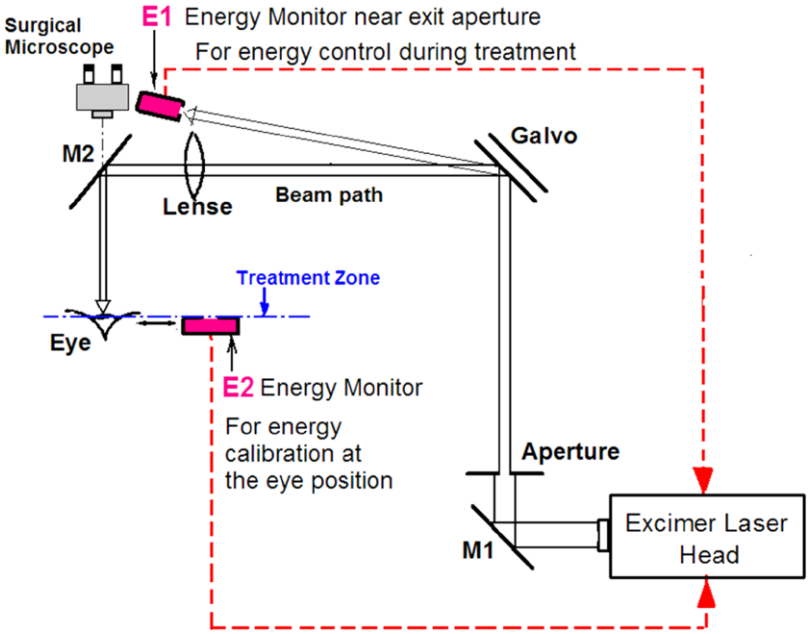

Figure 7. An optical scheme for an excimer-laser system 'MicroScan Visum'. A beam of an excimer laser is directed by a rotating mirror **M1** to mirrors of a galvanoscanner **Galvo**. Radiation is formed by the **Aperture** installed between the rotating mirror and the galvanoscanner. The mirrors of the scanner **Galvo** direct a laser beam through a lens **Lense** and a rotating mirror **M2** to the patient's **Eye**.

and high degrees of correction) the mathematical model was applied while planning surgery.

2.4.2. Physical simulation of ablation with a polymethylmethacrylate (PMMA) plate. To perform ablation, a PMMA plate was positioned in the place of an operated eye. After ablation, the plate surface was studied by a ZYGO scanning interference microscope. This provided an opportunity to find out the profile of energy density in a laser spot providing the maximum smoothness of the postsurgical surface (see below). Simulation with the plate also provided an opportunity to monitor the aberration quality of the obtained lenses and the stability of the pulse energy delivered to the surgical zone.

2.4.3. Laser spot size. The laser spot sizes from 0.7 to 1.14 mm were tested by mathematical simulation and in clinical practice. It was established that the spot size of 0.9 mm is sufficiently small for both high-quality standard and custom surgery. Reduction of the spot size lower than 0.9 mm makes the surgery take longer, but does not considerably affect the clinical results.

2.4.4. Shape of the energy profile in a laser spot. Due to special features of excimer lasers which have rectangular or irregular form of the output radiation beam, all commercial systems use a homogenization system and form the Gaussian profile for a scanning laser beam. Our research demonstrated, however, that in the case of scanning systems an almost flat profile of energy is optimal.

As one can see from figure 4, a flat beam almost does not have the zone of thermal heating at the residual cornea that prevents a pathological effect of surgery upon the residual tissue.

The thermal effect of the Gaussian beam over the residual tissue is visualized in the process of ablation on photographic paper, which contains gelatin similar to the properties of a

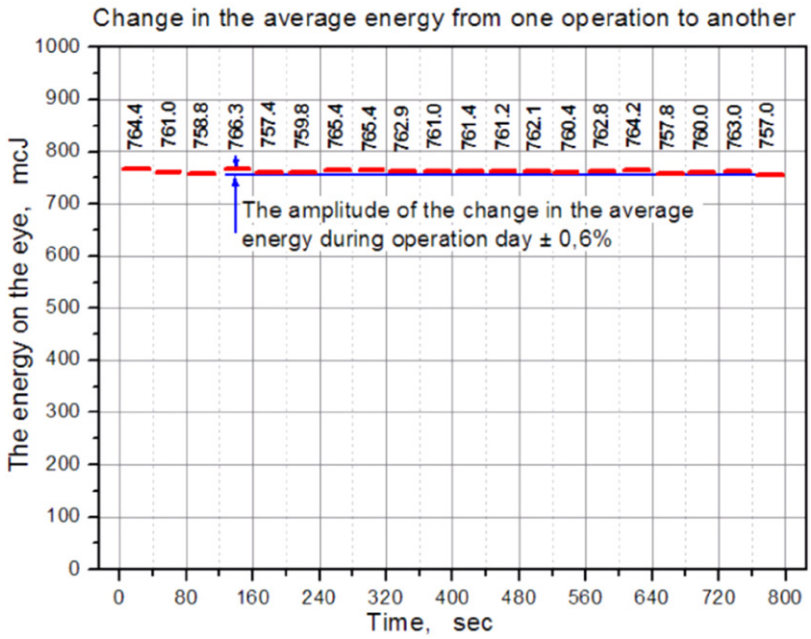

Figure 8. Energy dynamics of laser radiation during a surgery day with the 'MicroScan Visum' system (intervals between surgical operations are not shown).

cornea. A ring-shaped layer of carbonized gelatin is revealed around the ablation zone (figure 5). This is a clear indication of excessive overheating of the cornea in the case of the Gaussian beam.

Ablation by beams with flat and the Gaussian profiles were performed at a PMMA plate. The obtained shapes of the postsurgical surfaces were visualized using a ZYGO scanning interference microscope (figure 6).

Thus, the mean-square size of roughness for a flat beam is 2.3 times smaller than the roughness for the Gaussian beam.

Finally, visual monitoring by a surgeon using an operational microscope also verified a pronounced difference in the smoothness of the postsurgical corneal surfaces in favor of a flat profile.

2.4.5. Optical scheme and a system for energy stabilization in 'MicroScan Visum'. An optical scheme and a system for energy stabilization for 'MicroScan Visum' are given in figure 7.

An excimer laser CL-5000 from 'Optosystems, Ltd' [7] is used in the 'MicroScan Visum' system. There are two sensors for energy measurement in the system. The sensor **E1** measures energy continuously during surgery. It is located at the output aperture of the system. A surgical operation is divided into a short series of pulses. After each series, the beam is led out of the operation field and gets directed to the sensor **E1**. The laser high voltage is corrected according to the measurement results. This technique provides an opportunity to compensate absorption due to accidental emergence of an absorbing vapor (e.g. low-molecular spirits) in the optical tract.

The sensor **E2** is used for presurgical calibration of the system and is positioned at the place where an eye is located during surgery.

The quality of energy stabilizing in 'MicroScan Visum' was verified by simulating a surgery day consisting of 20 surgical operations needing 20 000 pulses each at the laser frequency of 500 Hz with 5 min intervals between the operations. Measurements were performed with an OPHIR pyroelectric sensor with a quartz diffuser. The energy of each of 20 000 pulses was written to a file and then averaged over 100 pulses. The result was presented as a text file.

The results of one of such set of measurements are displayed in figure 8.

One can see in figure 8 that the average energy deviation during a surgery day is 0.97% which corresponds to an error of 0.1 D in the case of a 10.0 D correction.

2.4.6. An eye-tracking system (A system of eye position monitoring). In the process of surgery, an eye cannot be fixed rigidly and, therefore, it continuously performs fast uncontrolled movements, both shift (with the amplitude up to several millimeters) and torsion (eye rotation around its optical axis with the amplitude of up to 10°). These movements need continuous automatic monitoring and the introduction of corresponding corrections to the surgical process, i.e. operation of and automatic ***eye-tracking system***.

The anatomical structures that the eye-tracking (monitoring) system may refer to are the following:

- a pupil
- an iris
- a limb (the boundary between an iris and a sclera).

Moreover, there is also an important nonanatomical reference point, i.e. the optical axis of an eye that is accessible for identification both at the stage of diagnostics by diagnostic equipment and in the 'MicroScan Visum' system at the stage of surgical treatment.

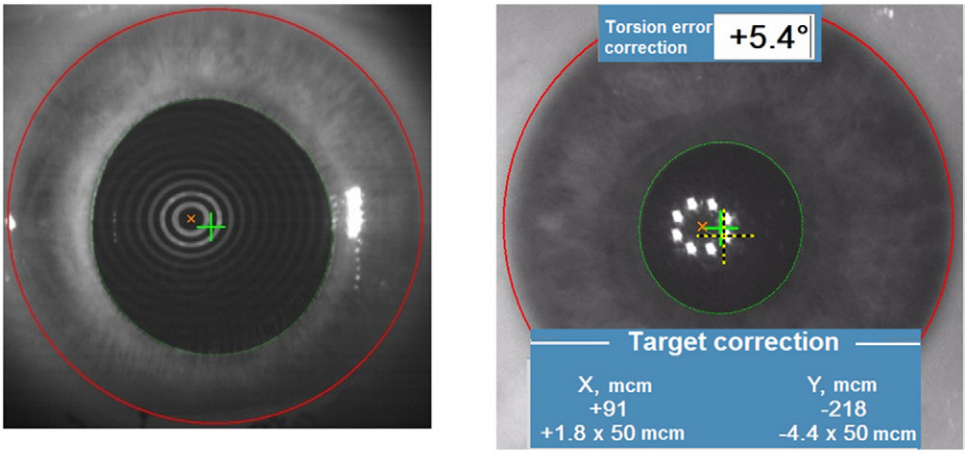

(a) (b)

Figure 9. Anatomical structures of an eye (a) at the diagnostic stage and (b) during surgery. (a) A diagnostic stage. Aberrometry in a dark room; the pupil is expanded. A green cross is the center of the expanded pupil. The center of the concentric circles is the eye's optical axis. (b) Surgery with 'MicroScan Visum'. A pupil gets narrower and shifts in the illuminated field of a surgical microscope. A green cross is the center of the narrow pupil. The center of 'eight dots' is the eye's optical axis. A yellow dotted line cross is the ablation center. It corresponds to the position of an expanded pupil during aberrometry.

The major problem for determination of eye position is the high physiological motility of a pupil and an iris. Figure 9 shows that in the process of surgery a pupil changes its shape and position in comparison with its state during diagnostics.

Since localization of the operation center (the center of the OZ) is determined at the diagnostic stage, it is necessary to transfer this information to the surgery stage. The limb is a stable anatomical structure and its position does not change while proceeding from the diagnostic stage to the surgery one. The position of the eye's optical axis (the point of its intersection with the corneal outer surface) can also be considered stable. By referring to the limb or the optical axis (according the surgeon's choice) the information on the operational center position is transferred from the diagnostic stage to surgery with 'MicroScan Visum'. Further tracking of the eye position during surgery can be performed (according to the surgeon's choice) according to both the limb and the pupil that may be considered stable during surgery.

The eye-tracking system implemented in 'MicroScan Visum' provides an opportunity to perform the whole scope of standard and custom surgical operations.

2.4.7. Prevention of corneal overheating. In the process of surgery, a part of the laser pulse energy may be transmitted to the tissues staying at the surgery location and cause pathological processes in them (burns and cell mutations). Therefore, experiments with the eyes of live rabbits were conducted using the systems 'MicroScan PIC' (the pulse frequency 100 Hz) and 'MicroScan Visum' (the pulse frequency 300 and 500 Hz), where surgical operations of PTC (phototherapeutic correction, i.e. removal of the constant-depth layer) type were performed. In this case, intraoperational temperature measurement was performed in the cornea by a Raytek Ti30 thermal imager. The maximum temperature increase in the cornea was detected for the 'MicroScan Visum' system at the pulse frequency of 500 Hz and it constituted 3.95 ± 0.75 °C (up to the temperature 34.97 ± 0.60 °C). This temperature increase in the cornea is physiologically harmless and close, for example, to the value of the analogous parameter for an excimer laser SCHWIND AMARIS (+3.73 °C) [8].

2.4.8. Ablation algorithm. A constructed mathematical profile for ablation must be implemented in the form of a sequence of coordinates for laser pulses at the cornea. The basis for the implemented algorithms is the principles of ***layerwise substance removal*** and ***minilensing***.

2.4.8.1. Layerwise removal of the cornea substance. Ablation of a cornea substance by layers of equal thickness (about 3 μm) is used in the 'MicroScan Visum' system. The size and shape of each layer depend on the ablation profile. Figure 10 presents the ablation algorithm of a cylindrical lens for myopia correction.

Each layer (referred to as a ***scan***) is formed as a hexagonal grid, where distances between the nodes are selected in such a way that laser spots with the centers in these nodes overlap (figure 11). In this case, each layer has its unique *XY* shift relatively to the first layer in order to provide additional smoothing for the postsurgical surface.

This provides surface smoothness after performing each single scan (figure 12).

2.4.8.2. Minilensing. In the case of the above-described layerwise removal of substance from the cornea during the whole surgical operation will have the shape of a pit with the bottom parallel to the presurgical corneal surface and only at the very end of the operation, a surface with the correct optical properties will be formed. If surgery is interrupted unexpectedly (a rare, but not impossible case), this geometry will produce sharp deterioration in vision in comparison with the presurgical state, the problem being that it is impossible to correct neither with spectacles, nor

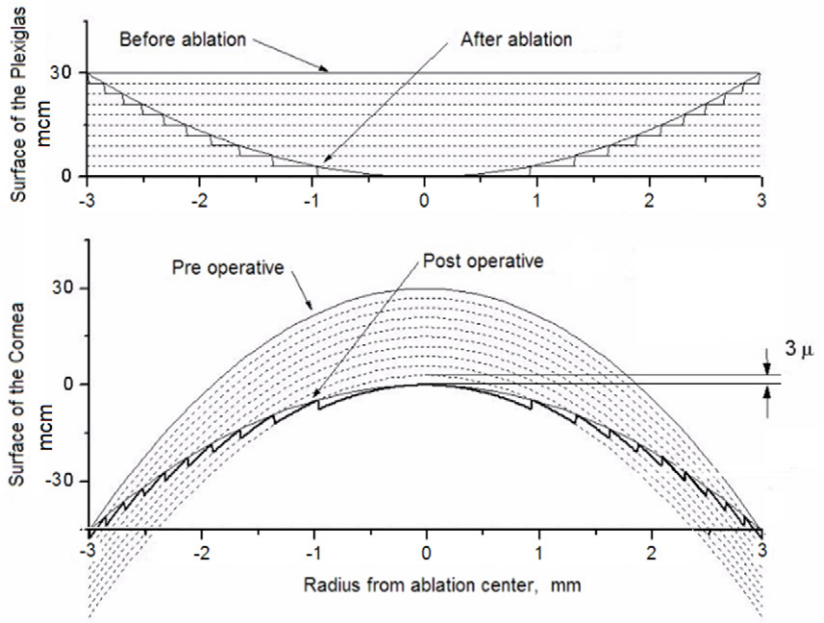

Figure 10. A principle of layerwise construction for the ablation profile at the flat surface of a PMMA plate (at the top) and at the convex surface of the cornea (at the bottom).

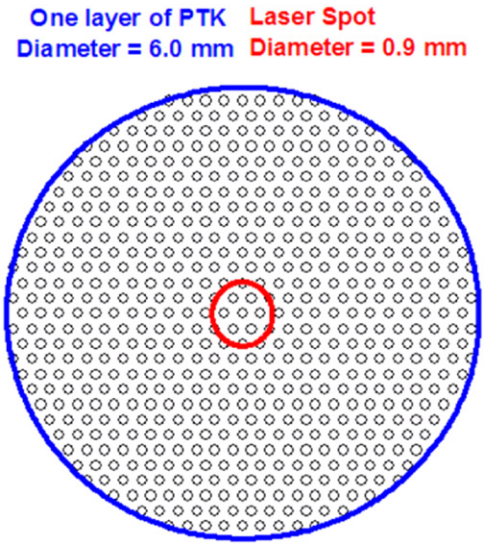

Figure 11. A scan with the hexagonal positions of the laser spot centers.

with regular surgery. It is certainly desirable in the case of an abrupt stoppage of surgery to have an absolutely different situation: not a disabled, but just an incompletely corrected eye, which might be completely corrected by one more regular operation.

To achieve this aim, the authors developed a technique of minilensing, i.e. such reordering of ablation layers (scans) that the strength of the optical correction will increase gradually, and at each moment of surgery the cornea will have almost correct optical properties.

Minilensing presumes reordering of ablation layers in the form of short sequences of 4–5 scans in such a way that each sequence forms a lens with very small optical strength at the cornea (a minilens). In this case, interruption of surgery at any moment means that only one minilens stays unfinished, while all the others have already been completely finished or have not yet been started. Only insignificant optical irregularity stays at the cornea in this case.

An example of minilensing is given in figure 13. The numbers near the layers in the upper part of the figure mean old numbers of scans (before minilensing).

2.5. A general functional diagram for the 'MicroScan Visum' system

The above-described principles and technological solutions were implemented in an excimer-laser surgical system. Its general scheme is given in figure 14.

2.6. Software

The surgical system is controlled by a special software in which calculation for standard types of surgical operations is incorporated, including the operations with a conical constant and tissue-saving ablation.

Surgery calculations for custom correction are implemented in our registered software packages 'KeraScan' (for corrections according to topograms) and 'PlatoScan' (for correction according to aberrometry).

2.7. Clinical results for different types of surgery

Surgery of all types described here is widely used in clinical practice. Altogether, over 500 000 surgical operations have been performed with the systems of the 'MicroScan' series during 15 years of its application. In the majority of cases, standard surgery correcting spheroastigmatic vision defects was conducted.

Custom surgery is applied for complicated cases of corneal defects, i.e. treating keratoconus, surgery after changes in corneal shape resulting from pathological processes, and

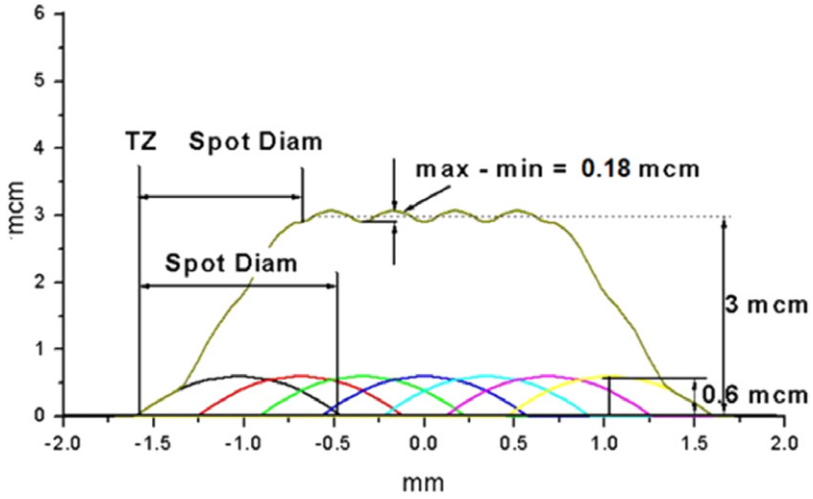

Figure 12. Laser spot overlapping in neighboring nodes.

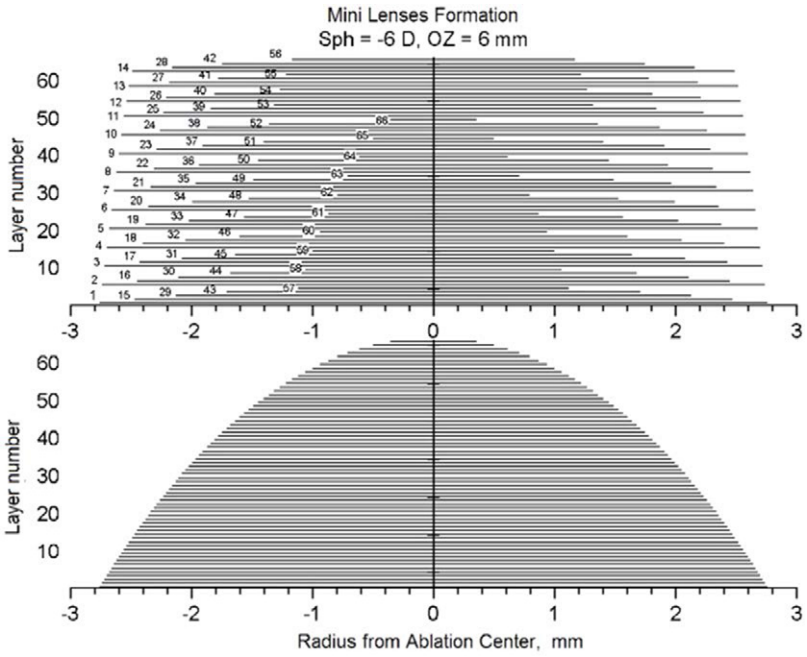

Figure 13. Minilensing in the case of myopia correction.

the correction of the consequences of unsuccessful surgery. However, custom surgery also demonstrates high results in the treatment of common spheroastigmatic vision defects (myopia and hyperopia + astigmatism).

In addition, we give a comparative analysis of the clinical results for surgery of two types:

(a) standard surgery performed with an excimer-laser system 'MicroScan Visum';
(b) custom surgery according to aberrometry data conducted at a combined platform including
- an excimer-laser system 'MicroScan Visum' with a software package for custom ablation 'PlatoScan';
- an aberrometer L-80 Wave+ software.

To compare the results of the two surgery types, we selected only surgical operations on myopia correction (of low, medium, and high degrees) by the LASIK technique, i.e. 114 operations of standard and 134 operations of custom types.

LASIK surgery was performed using a mechanical microkeratom 'Morya LSK One' with disposable heads. The flap diameter was 8–9 mm, and the thickness was 100 μm.

Refractive surgery was evaluated by the parameters of **predictability, efficiency, and safety**.

Predictability is the ratio of planned and achieved corrections for eye refraction.

The characteristic of surgical **efficiency** is the postsurgical acuity of vision measured with a standard Snellen-like diagnostic table, which provides an opportunity to determine the visual acuity with the step of 0.1 (letter recognition in each table line needs the visual acuity 0.1 higher than letter recognition in a previous line). Normal visual

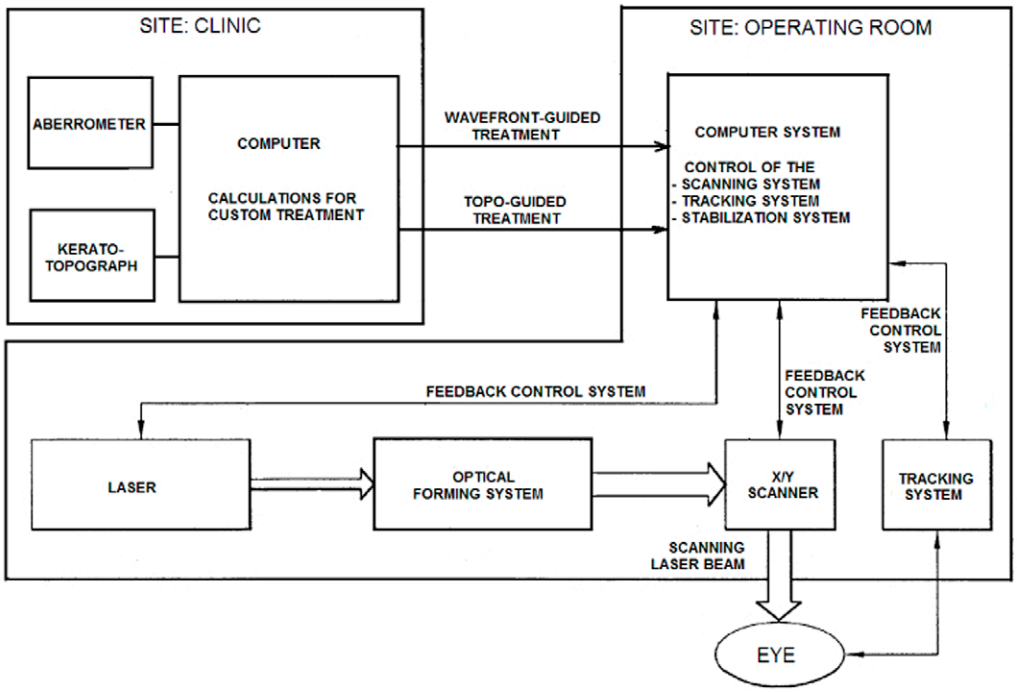

Figure 14. A general functional diagram for the 'MicroScan Visum' system.

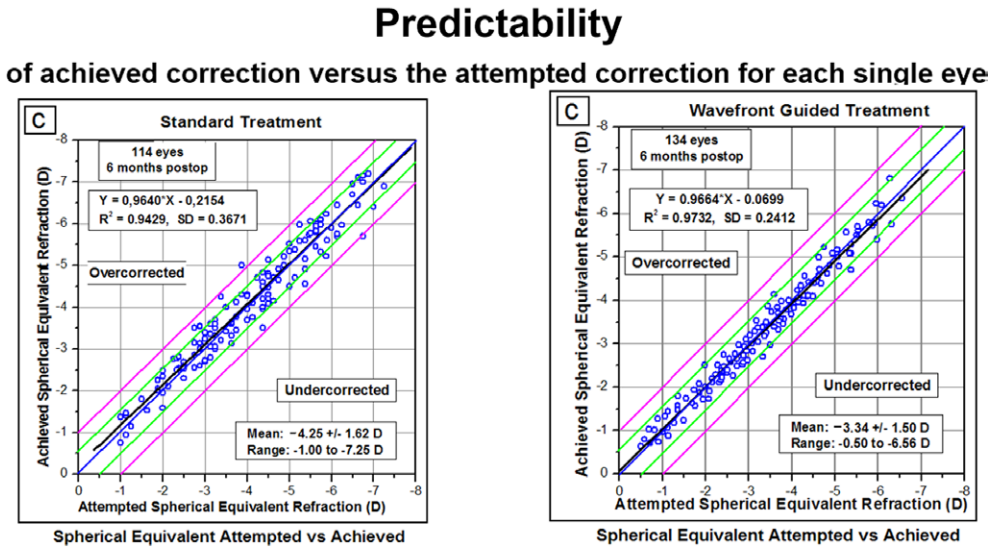

Figure 15. Scatter diagrams for planned and achieved spheroequivalent and plots for linear regression according to the correction results for myopic astigmatism in groups of standard (at the left) and custom (at the right) LASIK surgical operations.

acuity corresponds to the value 1.0. In clinical practice, the improvement or deterioration of vision not smaller than 0.1 is called a gain or loss of a corresponding number of lines in the checking table. The characteristic of surgical safety is the rate and clarity of vision deterioration resulting from a given type of surgery. The absence of visual acuity deterioration after surgery larger than 0.2 (two lines) is adopted as the **safety** standard.

A spheroequivalent, i.e. the half-sum of correction values for the corneal surface in two major meridians was selected as the characteristic of refractive correction for eyes, where myopia is combined with astigmatism (myopic astigmatism).

Predictability of the operations is illustrated in figure 15. The most appropriate cases of planned and achieved refractive coincidence are described by an equation $Y = X$ crossing the coordinate origin. The closer this line lies to the direct line of linear regression plotted according to a preset sample, the smaller are the values of under- or over-correction and the more predictable the results.

For both types of surgery:

- the inclination of a linear regression plot is close to 1.0 and varies from 0.94 to 0.97;
- the shift of a direct line for linear regression is smaller than 0.25 D.

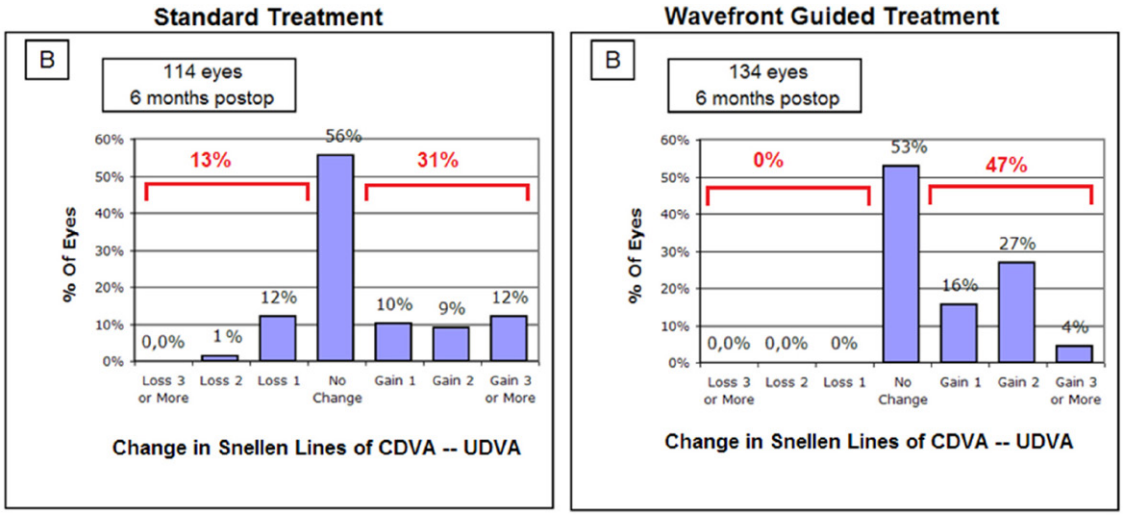

Figure 16. Comparison of uncorrected presurgical visual acuity with the maximum corrected presurgical visual acuity in groups of standard (at the left) and custom (at the right) surgical operations.

The average deviation from the achieved postsurgical results from the planned values does not exceed 0.25 D in the whole studied range from -1.0 to -8.0 D.

However, the mean-square and linear deviations from the regression line for the two surgery types differ more strongly:

- for standard surgery: $\sigma = 0.3671$ D, 72% of all surgical operations lie within the limits of ± 0.50 D from the direct line $Y = X$;
- for custom surgery: $\sigma = \pm 0.2412$ D, within the limits of ± 0.50 D from the direct line $Y = X$ for 92% of surgical operations.

Thus, aberrometry-based custom surgery provides much better precision of spheroequivalent correction that is realized clinically as a higher surgical efficiency.

We also compared the presurgical maximum corrected visual acuity for a large distance and the postsurgical uncorrected visual acuity for a large distance that was measured six months after surgery for the two indicated types of surgical operations. The results of this comparison are given in figure 16.

For the group of standard surgical operations, the postsurgical preservation of visual acuity or its increase with the gain of lines is observed for 87% of patients. For the group of custom surgical operations, the postsurgical preservation of visual acuity or its increase with the gain of lines is observed for 100% of patients without the line loss.

Thus, the custom surgery is more efficient than the standard one.

As for the safety parameter, the loss of visual acuity for more than two lines is not reported in any case for both surgery types, i.e. according to the above criterion the surgical operations of both types are safe for patients.

Thus, the clinical results are satisfactory for both standard and custom surgical operations. The above comparison demonstrates that custom aberrometry-guided surgery surpasses the standard one in all three clinical criteria (predictability, efficiency, and safety).

3. Femtosecond lasers

3.1. General issues for interaction of FS laser radiation with a substance

After their invention in the 1960s, lasers generating light pulses with a length shorter than several hundreds of femtoseconds found a large number of applications in technology, research, and medical science. Nowadays, FS lasers are used in the production of optical [9–12] (waveguides, caplers, and diffraction gratings) and liquid-based (microchannels, mixers, and chip laboratories) devices and also in medical science for the correction of corneal curvature (Small Incision Lenticule Extraction, SMILE) [14], the creation of a corneal flap [15], and cataract removal.

Commercially available lasers generate pulses of short length and provide an opportunity to attain significant peak intensities about 10 TW cm^{-2} in the case of strong focusing that makes FS lasers a unique instrument for intravolume processing of materials.

The first experiments on material processing with the help of FS lasers [16, 17] demonstrated an almost total absence of the thermal effect zone. In comparison with the use of nanosecond lasers, when thermal processes are dominant, the zone of thermal effect in the case of material processing by ultrashort pulses is insignificant, which provides an opportunity to use them for precise 3D processing of transparent materials. The time for excitation of an electronic subsystem is about several picoseconds, the time of electron thermalization is shorter than 100 ps, and the time of energy transfer to the lattice is 0.1–1 ns [18]. Thus, during the time of an FS pulse action only a small part of energy may be transferred to the lattice, the zones surrounding the interaction region, and on account of thermal diffusion. This makes material processing by FS pulses so precise.

In the process of irradiation, a laser pulse transfers energy to electrons through the processes of nonlinear ionization [19, 20]. The first experiments on intravolume processing of

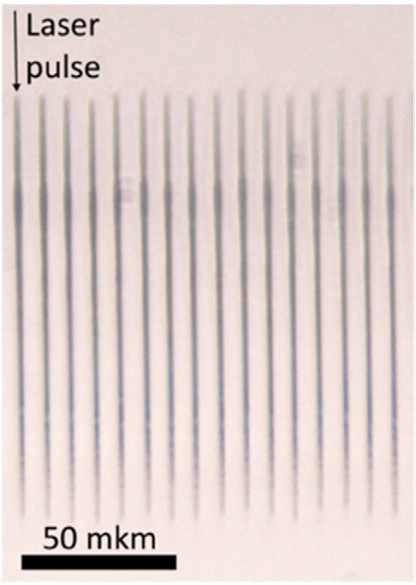

Figure 17. Extensive modifications within the volume of polycarbonate. Each modification (a cavity within polycarbonate) is produced under the effect of a single FS pulse.

materials [9] demonstrated that high intensities of laser pulses lead to strong nonlinear multiphoton absorption even in the transparent materials for the used wavelengths.

Apart from multiphoton absorption, a significant contribution to nonlinear ionization can be introduced by quantum tunneling of electrons from the valence band to the conductivity band.

At a laser pulse length within the range of several tens to several hundreds of femtoseconds, the initial free electrons excited in the process of multiphoton absorption can absorb a considerable part of the pulse energy. In the case of acquiring a certain value of kinetic energy, they (in a collision) can excite electrons in the valence band and initialize cumulative ionization. The achievement of excited electron density of about 10^{29} m^{-3} leads to plasma formation in the effect zone of an FS pulse [19].

In the case of focusing of FS pulses within the volume of a transparent material, the necessary conditions for nonlinear ionization are created only in a small region of a focal volume. The plasma formed under the effect of FS pulses may lead to various types of internal material modifications like variation of the refractive index [13, 21], a rise in birefringence [22, 23], microdestruction [24], and various types of photoconversion [25, 26]. Strong nonlinear multiphoton absorption and almost complete absence of the thermal effect zone provide an opportunity to achieve the micrometer-scale spatial resolution of processing.

In the ideal case, a focused FS pulse produces a spherical modification within a volume with the diameter of several micrometers (typically, smaller than 2 μm). However, in the majority of cases the modification region differs considerably from a sphere and is shaped as ellipses elongated along the direction of radiation propagation. There are several reasons for these deformations. One of the most important ones is the Kerr self-focusing (SF). A high peak power of a laser pulse may exceed the threshold of light SF in a medium and lead to an additional focusing of radiation and its filamentation [27]. This forms within the material volume an extensive modification (figure 17) with the constant diameter of several micrometers and the length exceeding tens of micrometers [26]. The process of radiation filamentation in transparent materials and theoretical models for radiation propagation in the case of SF are considered in detail in [28]. This effect is especially strong at relatively small numerical apertures of focusing systems. Its influence is reduced noticeably in the case of pulse focusing by wide-aperture lenses or when varying the intensity distribution of a focused pulse [26].

As was demonstrated in [29], a considerable effect upon the intensity distribution in the focal waist can be produced by the inherent spherical aberration of a lens and the interface spherical aberration (ISA) connected with the transition of radiation between optical media with different refractive indices. The first effect can be compensated successfully by the selection of focusing optics. The ISA arising at radiation focusing through the boundary of refractive indices 'air—sample' is difficult to eliminate. Specially calculated focusing systems are needed to suppress it. ISA leads to the elongation of the modification region formed by an FS pulse from the region of the geometrical focus in the direction of radiation propagation [26, 29]. Volume modifications of polycarbonate with the aspect ratios (diameter/length) over 100 were obtained in [26], and the reason for elongation was ISA.

While processing transparent dielectrics, it is necessary to also take into account some other effects, e.g. nonlinear propagation of pulses through focusing optics [30].

Apart from the above effects in the case of the intravolume processing of transparent materials with significant overlapping of focusing spots at scanning, a considerable influence can be produced by the effects of thermal accumulation [10, 31], self-induced shift of a focusing spot [26], and some others.

The advantages of FS laser application are the opportunity to process intravolume regions without affecting the regions around the action zone, a high degree of micromodification localization, and the absence of a thermal action zone, which are crucial for their use in medical science, in particular in ophthalmology.

3.2. Ophthalmological FS laser systems

At present, the application of FS lasers is expanding rapidly in ophthalmology. The technological basis is the intrastromal processing of the cornea, where a FS laser beam is focused sharply into the internal layers of the cornea and a local dissection of the cornel layers is performed. At present, FS lasers are used for the following types of surgery.

3.2.1. FemtoLASIK. FemtoLASIK surgery consists of two stages. At the first stage, a corneal flap with a thickness about 100 μm is formed with the help of a FS laser (figure 18(1)). This flap contains epithelium, which is not affected by the laser at the second stage, and this improves the predictability of results and the postsurgical rehabilitation. Then, the obtained flap is separated with the help of a special instrument

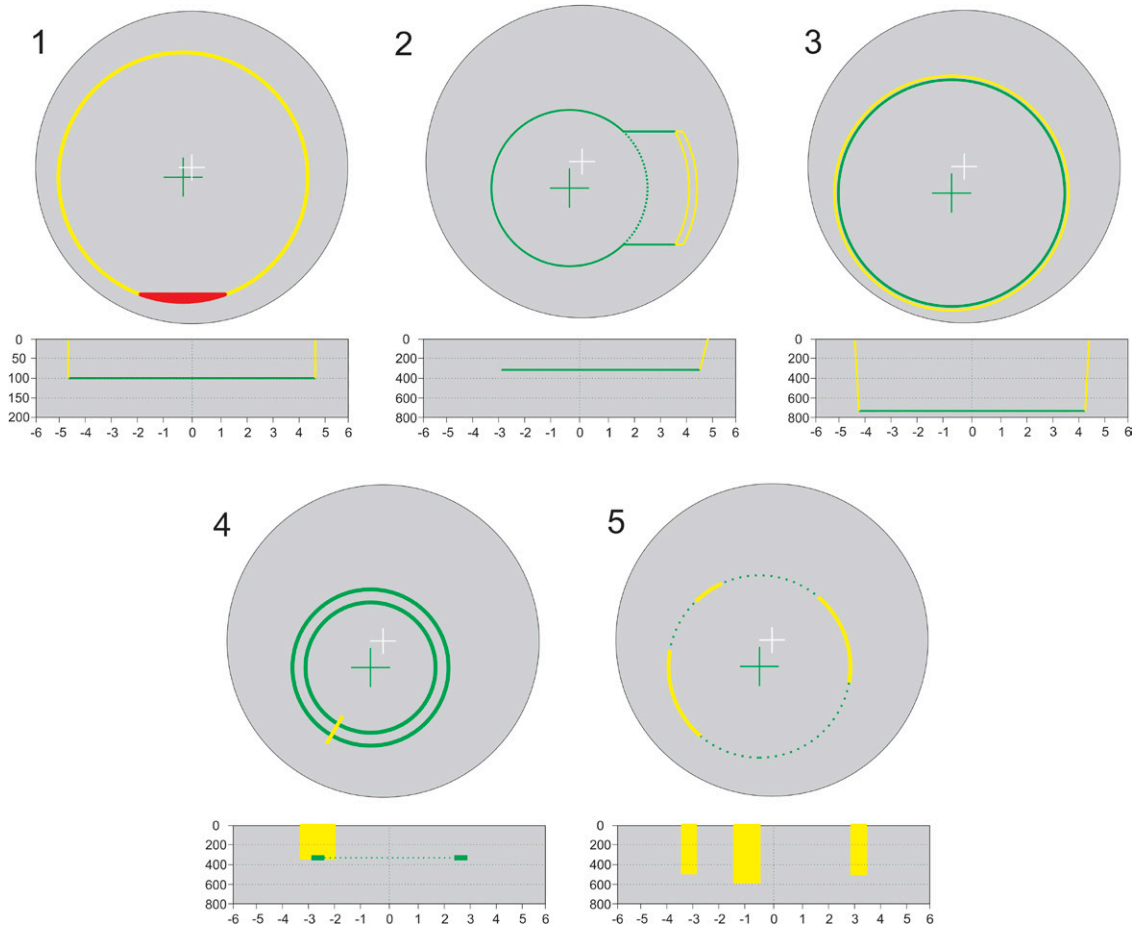

Figure 18. Surgery types available with an ophthalmological 'FemtoVisum' system. 1—femtoLASIK; 2—a corneal pocket; 3—keratoplasty; 4—a corneal tunnel; 5—arcuate incisions.

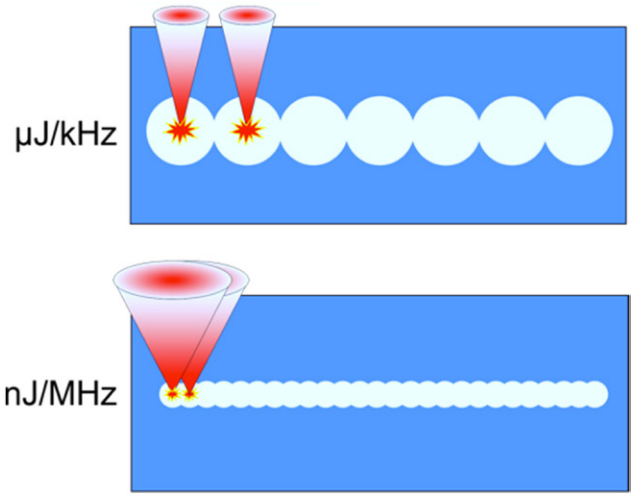

Figure 19. Illustration for different approaches and algorithms for the process of corneal incision formation with the help of FS laser pulses.

from the major part of the cornea in such a way that it does not cover the corneal optic zone. At the second stage, the patient's cornea is affected by an excimer laser forming the necessary curvature of the corneal surface. After that, the corneal flap is returned to its place.

3.2.2. Formation of corneal pockets (figure 18(2)). In the case of a thin cornea, a disease called keratoconus is frequently encountered, when the internal pressure of an eye presses out the cornea, resulting in complete loss of vision. To increase the mechanical properties and correct the corneal curvature, a plastic ring is installed into the stroma or a special strengthening solution is infused. A FS laser makes an incision at a preset depth in the center of the optic zone with a narrow outlet at the corneal surface for ring or solution introduction. Also, a small (up to 3 mm) lens may be introduced through such an incision made by a FS laser to correct presbyopia, which plays the role of spectacles for reading in senior patients. The advantage of this surgery is an opportunity to change the lens quickly under surgical conditions.

3.2.3. Keratoplasty (transplantation of the cornea). To transplant a cornea it is necessary for the donor material and the patient to be operated on using one and the same FS laser system, since stringent requirements exist for the shape and dimensions of a donor corneal flap and bed for the patient (figure 18(3)). Keratoplasty may be both through the front and rear, when the patient's cornea is removed for the whole depth, and through the front or rear, when only the upper or lower part of it is removed, respectively. During an operation the surgeon using a FS laser cuts the necessary flap in

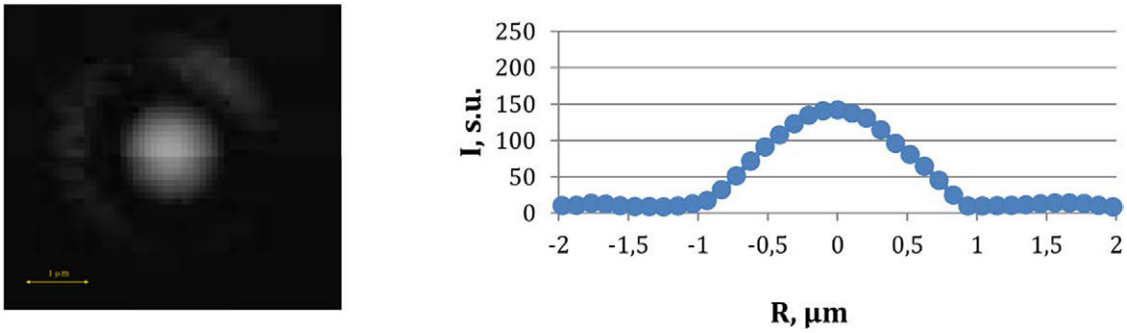

Figure 20. A spatial intensity distribution for a focal spot in air at a normal incidence.

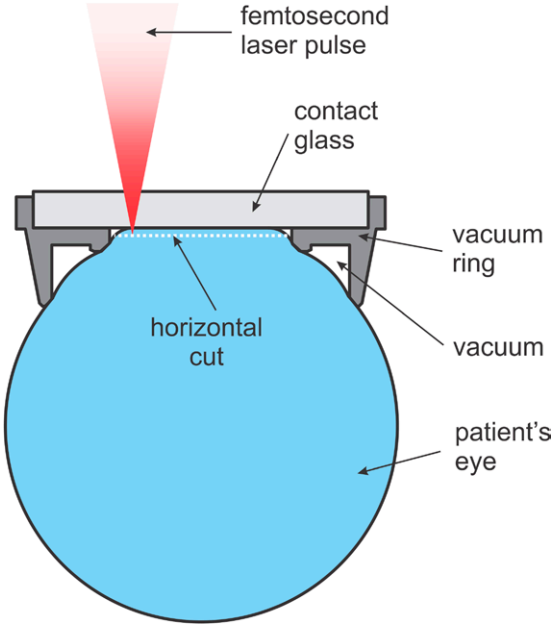

Figure 21. A horizontal cut (a laser beam moves along two coordinates X–Y).

the donor material. Then, he repeats this operation with the patient, forming a corneal bed. After that, the surgeon puts the flap into the bed and joins them together.

3.2.4. Formation of a corneal tunnel for introduction of segments to the peripheral zone of the cornea and also the introduction of riboflavin to strengthen the cornea. A tunnel with a small cut to the surface is formed in the stroma at a preset depth with the help of a FS laser (figure 18(4)). Different from a corneal pocket, in this case the optic zone stays intact. After tunnel formation the surgeon uses a special instrument to introduce plastic segments through the cut. After the operation, the surgeon sutures the cut, if necessary.

3.2.5. Arcuate incisions of the cornea for correction of astigmatism or access to the anterior chamber of the eye (figure 18(5)). In this case, a laser is used as a precision surgical knife. In the process of incision, the internal eye pressure slightly opens the incision, changing the corneal curvature in this way in the direction perpendicular to the incision.

3.2.6. Correction of refraction using a FS laser only. A lenticule with a known curvature of surface is formed by a laser in the corneal stroma in this case. Furthermore, it is taken out through an incision in the cornea.

3.2.7. Destruction of the lens nucleus in the case of a cataract.

3.2.8. Capsulorhexis that is a precision opening of the lens capsule in the eye for further extraction of the lens nucleus through an obtained window.

3.2.9. Versions for laser processing of the cornea. Two approaches are possible in intrastromal processing of the cornea:

- application of a laser with relatively high pulse energy (over 1 μJ) and a relatively low repetition rate (30–200 kHz). A conditional name of this mode is μJ/kHz.
- application of a laser with relatively low pulse energy (smaller than 1 μJ) and a high repetition rate (over 500 kHz). A conditional name for this mode is nJ/MHz.

Different approaches to the algorithm of laser focal spot motion in corneal internal layers are necessary to implement the mode of corneal cutting (dissection) depending on the selected laser and effect types (nJ or μJ). By virtue of the specific character of the physical processes occurring at different laser parameters the results of processing depend strongly on both a spatial location and sequence of action (a cumulative effect) upon this region of a biological material. Figure 19 demonstrates schematically the versions for such interaction and the difference in the obtained results, i.e. a narrower cut and a smoother configuration of edges in the case of the nJ/MHz mode with a small focusing spot.

3.3. An ophthalmological FS laser system 'FemtoVisum'

To achieve the best clinical results we selected the nJ/MHz mode in the process of development of the 'FemtoVisum'. We used an objective lens (NA = 0.3) of our own design for the 'FemtoVisum' system. It provides a 2 μm focusing spot in the corneal depth. The objective visual field provides an opportunity for angular scanning by a laser beam over the frame >200 μm. In the developed multiple-lens objective, a possibility for changing the focus at shifting of one of its lenses is provided

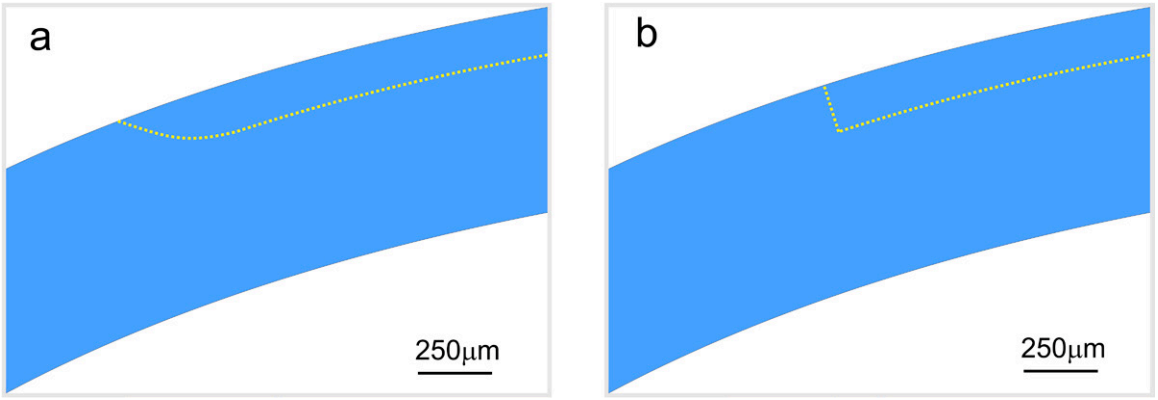

Figure 22. A flap shape depending on the mode of the laser beam scanning: (a) a horizontal cut only and (b) a laser cut with vertical scanning.

at constant focusing quality. Figure 20 demonstrates an image for the focal point and an intensity distribution.

We used a FS optical-fiber laser FL300 of our own design as a radiation source. At the laser pulse rate of 1 MHz, the pulse energy attains 2 μJ, which allows us to implement the nJ/MHz mode at a double reserve in pulse energy. The generation pulse length for an FL300 laser is smaller than 300 fs and the generation wavelength is 1040 nm.

The mode of beam scanning within the cornea for a FS laser is an essential issue for the implementation of various microsurgical ophthalmological technologies. Figure 21 shows the way for LASIK surgery at laser beam scanning in only one plane. In this case, a laser beam leaves the cornea in an open space in a horizontal plane. In this connection, the edge of the corneal flap is wedge-shaped (figure 22(a)). In the case of vertical beam scanning, it is possible to produce a corneal flap with vertical walls (figure 22(b)) and in a general case, with an arbitrary inclination of the flap edge.

As a rule, in the case of LASIK surgery, the diameter of the processed corneal zone for a patient's eye must be not smaller than 9.5 mm. The operational field for the micro-objective lens of our design is 200 μm. In the developed system, the whole cut field with the diameter up to 10 mm was 'covered' by sections of 200 μm.

To cover the whole operational field uniformly by a micro-objective lens with the field up to 200 μm, we used angular scanning over one coordinate Y (see figure 23). Scanning was performed by a resonance galvanoscanner with the scanning frequency of 8 kHz. We used the optical scanning angles not exceeding 1°. This provided an opportunity to obtain the width of the angular scanning over a field larger than 200 μm, i.e. to cover the operational field of the objective completely. In this case, the distance between the neighboring spots (from each laser pulse) was smaller than 5 μm.

The objective lens was positioned at a movable (in the plane perpendicular to a laser beam) platform moving along the X and Y axes. A fast motion along the X axis together with angular scanning provided a scanning band with the density of filling by laser pulses determined by the motion velocity. Transition from one band to another was performed using the coordinate Y of the movable platform. Thus, the

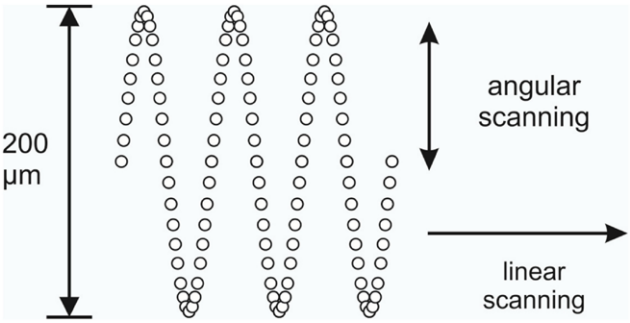

Figure 23. Angular scanning with linear sweep.

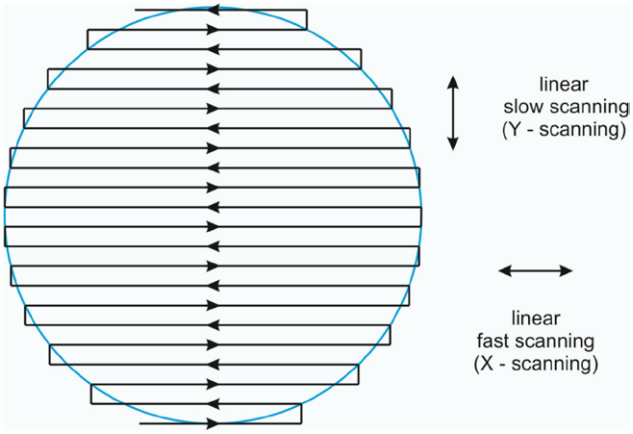

Figure 24. A pattern of linear scanning.

linear scanning was performed within the whole cut region (figure 24).

The critical role for the final result belongs to the uniformity of the filling of the whole cut area by laser pulses, because of the presence of the cumulative effect from almost spatially coinciding laser pulses. For this, we use several patented methods [32] such as motion linearization and the technology 'Smooth Lines' of our design (figure 25).

To linearize motion, we used an acousto-optic modulator (AOM). It was used to eliminate pulses located at the sinusoid peaks. Thus, only the sections with linear motion remained.

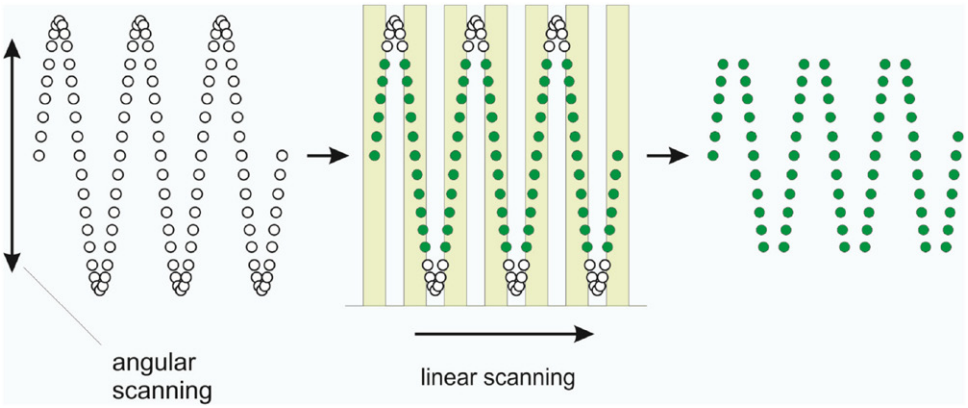

Figure 25. Schematics for the method of motion linearization and the technology 'Smooth Lines' in the 'FemtoVisum' system.

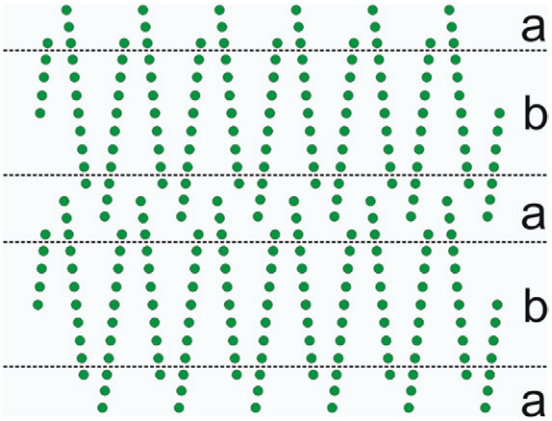

Figure 26. Schematics for the technology 'Smooth Lines' used for the seamless junction of the scanning bands.

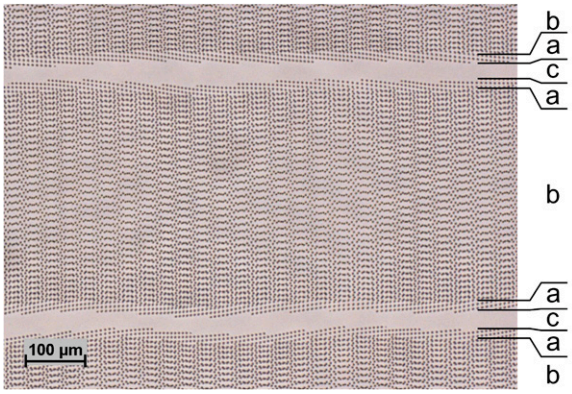

Figure 27. A part of the polycarbonate plate after microprocessing by a FS laser. The width of a scanning band is 400 μm, the distance between the band centers is 430 μm, and the velocity of the linear scanning is 60 mm s^{-1}. Numbers indicate different zones: (a) a transition zone arising due to asymmetric cutting of the scanning bands (the technology'Smooth Lines'); (b) the basic part of a scanning band; and (c) a gap between the scanning bands (deliberately set nonzero).

The technology 'Smooth Lines' was developed for a seamless junction of scanning bands. The point is that the distance between the bands is not the same and they are either at a certain distance from each other (forming in this way a zone not processed by a laser) or overlap (forming a zone of excessive laser processing). However, in the case of asymmetric cutting of scanning bands by AOM, it becomes possible to create a transition zone between the scanning bands and that is the concept of the 'Smooth Lines' technology (figures 26 and 27). The presence of the transition zone allows us to improve the uniformity of the microprocessing.

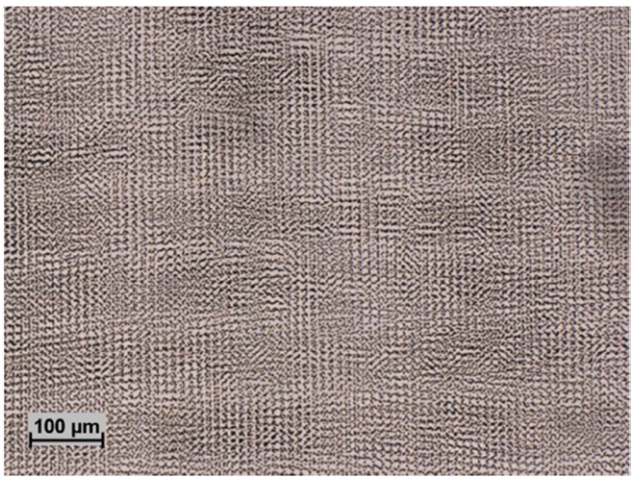

Figure 28. A part of a polycarbonate plate after microprocessing by a FS laser. The width of a scanning band is 400 μm, the distance between the scanning band centers is 100 μm, and the velocity of the linear scanning is 100 mm s^{-1}.

Figure 27 shows a single scanning band. One can see that the density of pulses increases from the band center to its edge, but it stays almost the same at the central 200–250 μm. If the bands get closer, the transitions zones overlap forming a seamless junction.

To increase the processing uniformity further, we used re-overlapping of the scanning bands. In this case, 2–4 scanning bands are located in any part of the processed surface. Figure 28 demonstrates a surface part with four-times re-overlapping. In this case, the average distance between the pulses is smaller than 2 μm and there are no regions with the distance between pulses smaller than 5 μm, but there is no cumulative effect since the pulses close to each other are strongly separated in time (~100 ms).

The 'FemtoVisum' system combined with 'MicroscanVisum' forms a laser-ophthalmological complex (figure 29). It provides an opportunity to solve the whole

Figure 29. An ophthalmological complex Visum ('FemtoVisum' at the left and 'MicroscanVisum' at the right) in the MNTK Cheboksary.

scope of problems on vision correction by treating an eye cornea with laser radiation [33].

The key advantages of using the FS laser system 'FemtoVisum' in ophthalmology is reproducibility and precision of surgery (the flap thickness, the depth of cuts, and the size and shape of a transplant at keratoplasty), a short time of surgery (<15 s for a flap with the diameter of 9.5 mm in the case of LASIK surgery), and a wide scope of possible surgical operations (femtoLASIK, a corneal pocket, keratoplasty, corneal tunnels, and arcuate cuts).

At present, the 'FemtoVisum' system is registered as a medical device and is being applied successfully in many hospitals [34–37].

References

[1] Trokel S, Shrinivasan R and Braren B A 1983 Excimer laser surgery of cornea *Am. J. Ophthalmol.* **96** 710–5

[2] Atejev V V, Bukreyev V S, Vartapetov S K, Semenov A D, Sugrobov V A, Turin V S and Fedorov S N 1999 Excimer laser system «Profile-500» *ALT'98 Selected papers on Novel Laser Methods in Medicine and Biology, SPIE* vol 3829 pp 124–7 (paper 3829–19)

[3] Lin J T and LaserSight Inc. 1996 Ophthalmic surgery method using non-contact scanning laser *US Patent* 5520679

[4] Борн М and Вольф Э 1973 *Основы оптики* (Москва: Наука) pp 703–7

[5] Thibos L N, Applegate R A, Schwiegerling J T, Webb R, Memebers V S T 2000 Standards for reporting the optical aberrations of eyes *Vision Science and its Applications* ed V Lakshminarayanan (Washington, DC: Optical Society of America)

[6] Jiménez J R *et al* 2005 Correction factor for ablation algorithms used in corneal refractive surgery with Gaussian-profile beams *Opt. Express* **13** 336–43

[7] www.optosystems.ru/en/excimer-lasers/

[8] 2010 Thermodynamic measurements confirm high safety of the SCHWIND AMARIS' *Intelligent Thermal Effect Control* (Kleinostheim, Germany, April 2010: Schwind Press Release)

[9] Davis K M, Miura K, Sugimoto N and Hirao K 1996 *Opt. Lett.* **21** 1729–31

[10] Eaton S M, Zhang H, Herman P R, Yoshino F, Shah L, Bovatse K J and Arai A Y 2005 *Opt. Express* **13** 4708–16

[11] Chan J W, Huser T R, Risbud S H and Krol D M 2003 *Appl. Phys.* A **76** 367–72

[12] Cheng Y, Sugioka K, Masuda M, Toyoda K, Kawachi M, Shihoyama K and Midorikawa K 2003 *RIKEN Rev.* **50** 101

[13] Cheng Y, Sugioka K, Midorikawa K and Xu Z 2006 *SPIE Newsroom* http://spie.org/x8513.xml

[14] Reinstein D Z *et al* 2014 Oct 16 *Eye and Vision 1:3*

[15] Vartapetov S K, Khudyakov D V, Lapshin K E, Obidin A Z and Shcherbakov I A 2012 *Kvantovaya Elektron* **42** 262

[16] Srinivasan R, Sutcliff E and Braren B 1987 *Appl. Phys. Lett.* **51** 1285–7

[17] Küper S and Stuke M 1987 *Appl. Phys.* B **44** 199–204

[18] Gattass R G and Mazur E 2008 *Nat. Photon.* **2** 219–25

[19] Stuart B C, Feit M D, Rubenchik A M, Shore B W and Perry M D 1995 *Phys. Rev. Lett.* **74** 2248–51

[20] Stuart B C *et al* 1996 *Phys. Rev.* B **53** 1749–61

[21] Miura K, Qiu J R, Inouye H, Mitsuyu T and Hirao K 1997 *Appl. Phys. Lett.* **71** 3329

[22] Sudrie L, Franco M, Prade B and Mysyrowicz A 1999 *Opt. Commun.* **171** 279

[23] Hnatovsky C, Taylor R S, Rajeev P P, Simova E, Bhardwaj V R, Rayner D M and Corkum P B 2005 *Appl. Phys. Lett.* **87** 014104

[24] Schaffer C B, Brodeur A, Garcia J F and Mazur E 2001 *Opt. Lett.* **26** 93–5

[25] Morita N, Shimotsuma Y, Nishi M, Sakakura M, Miura K and Hirao K 2014 *Appl. Phys. Lett.* **105** 201104

[26] Ganin D, Obidin A Z, Lapshin K and Vartapetov S K 2015 *Quantum Electron.* **45** 725–30

[27] Couairon A, Sudrie L, Franco M, Prade B and Mysyrowicz A 2005 *Phys. Rev.* B **71** 125435

[28] Couairon A and Mysyrowicz A 2007 *Phys. Rep.* **441** 47–189

[29] Sun Q, Jiang H, Liu Y, Zhou Y, Yang H and Gong Q 2005 *J. Opt. A: Pure Appl. Opt.* **7** 655–9

[30] Dergachev A A, Ionin A A, Kandidov V P, Mokrousova D V, Seleznev L V, Sinitsyn D V, Sunchugasheva E S, Shlenov S A and Shustikova A P 2015 *Laser Phys. Lett.* **12** 1

[31] Schaffer C, Garcia J and Mazur E 2003 *Appl. Phys.* A **76** 351–4

[32] Borodkin A A, Vartapetov S K, Lapshin K E and Obidin A Z Laser scanning system based on a resonance scanner RU 2492514 C1

[33] Kishkin Yu I and Tahchidi N Ch 2013 Effectiveness of the *Q*-value guided femto-lasik Femto-Visum *Bull. Orenburg State Univ.* **4** 135–8

[34] Kishkin Yu I, Lapshin K E, Nikolaev D P, Kononenko A A and Makarov A V 2011 Femto VIZUM—Russia's first femtosecond laser in clinical practice *Modern Technologies in Cataract and Refractive Surgery—2011, Proc. (Moscow)* pp 330–2

[35] Mushkova I A, Kishkin Yu I and Takhchidi N Kh 2013 Comparative analysis of ophthalmo-ergonomic data after femtosecond laser-assisted Femto-Lasik and Femto-Visum *Bull. Orenburg State Univ.* **4** 2, 181–3

[36] Doga A V, Vartapetov S K, Mushkova I A, Kishkin Yu I, Maychuk N V and Kechin E V 2015 Long-term clinical and functional outcomes of refractive errors correction by the first domestic femto laser system FemtoVizum *Mod. Technol. Ophthalmol.* **4** 185

[37] Pashtaev N P, Pateeva T Z, Kulikova I L and Pozdeeva N A 2015 Early results of myopia correction with domestic femtosecond laser Femto Vizum *Mod. Technol. Ophthalmol.* **4** 116